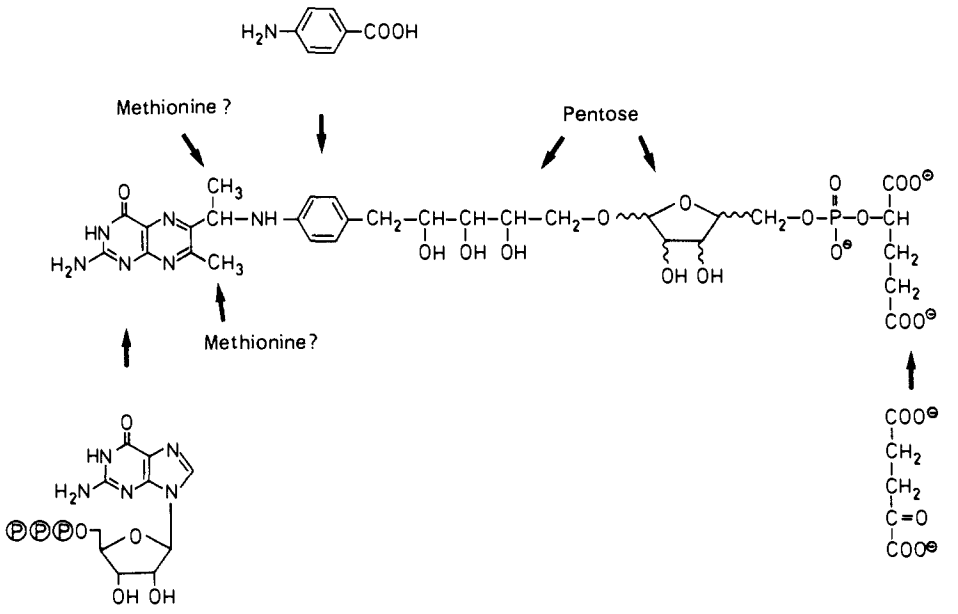

Figure 2. Hypothetical building blocks of methanopterin.

pentityl side chain of the aniline moiety. With these assignments at hand, we obtained the relative ^{13}C abundances shown in Figure 1 (numbers in boxes). Carbon atoms without designation had relative abundances of 0.8–1.2. It is immediately apparent that the metabolism of acetate in *M. thermoautotrophicum* proceeds almost without randomization of the isotope in agreement with our earlier findings.[5]

Comparison of guanosine and methanopterin shows that, as expected, the pentose moieties have exactly the same labeling patterns in both molecules. The labeling patterns of the heterocyclic moieties confirm that the pyrimidine ring of methanopterin is derived from a purine precursor in analogy with the biosynthesis of folic acid and unconjugated pteridines.

The origin of the pyrazine ring in methanopterin is less obvious. A ring expansion in analogy to folate biosynthesis would correctly predict the labeling of position 7a which should be derived from the labeled C-1′ of a purine nucleotide, presumably GTP. This would imply that the methyl group at C-7a is introduced into the pteridine system by secondary methylation, e.g., from methionine as donor.

We can rule out the possibility that both carbon atoms of the alkyl side chain at C-6a are derived from the ribose moiety of the purine nucleotide, with removal of the terminal carbon, because C-12a, which would then originate from the labeled C-4 of a pentose, is not enriched. We propose that the pyrazine moiety is formed by the classical ring expansion, and the C-6 substituent is subsequently either shortened by two carbon atoms or removed entirely, with subsequent introduction of one or two carbon atoms from a hitherto unknown source. This question requires additional experimentation.

A comparison of the aniline moiety of methanopterin with tyrosine shows a very similar labeling pattern clearly suggesting that the aromatic ring is derived from the shikimate pathway. It is also apparent that the ^{13}C-enriched side-chain atom C-1c is not derived from either the carboxyl group of shikimic acid or C-3 of pyruvate, via chorismate, since both should be unlabeled. On the other hand, the labeling pattern of the pentityl side chain is in full agreement with that of a pentose. We therefore suggest that the pentitylaniline moiety arises from the ring carbon atoms of a shikimate derivative, e.g., 4-aminobenzoate, and a pentose chain incorporated in its entirety. Mechanistic precedent for such an origin exists, e.g., in the formation of indoleglycerol phosphate from phosphoribosylanthranilate in tryptophan biosynthesis. The suggested pathway again requires confirmation by additional experiments.

Finally, the labeling pattern of the hydroxyglutarate moiety is exactly as expected if this moiety is formed by reduction of 2-ketoglutarate. Ketoglutarate should originate from acetate by three steps of reductive carboxylation via pyruvate, oxaloacetate, and succinate. The symmetry of succinate would lead to the equal distribution of the isotope between positions 3e and 4e.

The above results establish most of the building blocks of methanopterin as summarized in Figure 2.

Acknowledgment. This work was supported by grants from the Deutsche Forschunsgemeinschaft and the Fonds der Chemischen Industrie to A.B., from NIH (GM 32910) to H.G.F. and P.J.K., and from NATO to A.B. and P.J.K. We thank Prof. R. S. Wolfe, University of Illinois, Urbana, for a reference sample of methanopterin. We also thank Angelika Kohnle and Astrid König for help with the preparation of the manuscript.

Nucleophilic Catalysis of the Migratory Insertion of Carbon Monoxide. Evidence for a Dissociative Trapping Mechanism

Steven L. Webb, Christen M. Giandomenico, and Jack Halpern*

Department of Chemistry, The University of Chicago Chicago, Illinois 60637

Received September 3, 1985

Migratory insertion of carbon monoxide into transition-metal alkyl bonds constitutes one of the most fundamental and extensively investigated reactions in organometallic chemistry and homogeneous catalysis.[1] Several earlier studies have described marked enhancements of the rates of such migratory insertion reactions by nucleophilic solvents or catalysts (S) and have interpreted these enhancements in terms of the mechanistic scheme of eq 1 and 2.[2,3] This interpretation ascribes the catalytic influence

$$L_nM(CO)R + S \rightleftarrows L_nMC(=O)R(S) \quad (1)$$

$$L_nMC(=O)R(S) + L' \rightarrow L_nL'MC(=O)R + S \quad (2)$$

$$L_nM(CO)R + L' \xrightarrow{S} L_nL'MC(=O)R \quad (3)$$

of the nucleophile S to stabilization of the coordinatively unsaturated intermediate that is generated by the migratory insertion

(1) Kuhlmann, E. J.; Alexander, J. J. *Coord. Chem. Rev.* **1980**, *33*, 195 and references therein.
(2) Mawby, R. J.; Basolo, F.; Pearson, R. G. *J. Am. Chem. Soc.* **1964**, *86*, 3994.
(3) Wax, M. J.; Bergman, R. G. *J. Am. Chem. Soc.* **1981**, *103*, 7028.

0002-7863/86/1508-0345$01.50/0

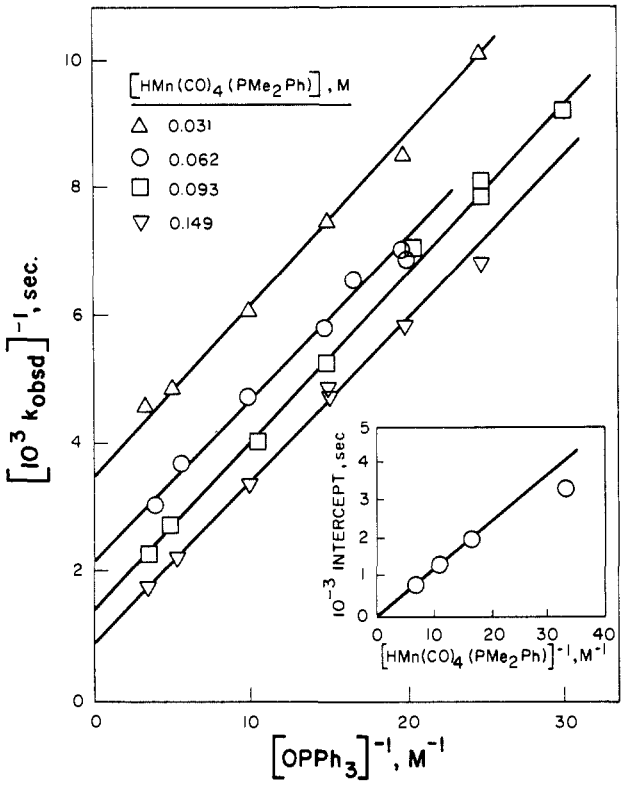

Figure 1. Kinetic data for reaction 4 in C_6D_6 at 45 °C plotted according to eq 13.

of CO, by coordination to the vacant coordination site.

A persistent troubling feature of this interpretation has been that if a vacant coordination site is required for trapping of the acyl intermediate by L′, why is the trapping facilitated when this coordination site is occupied by the nucleophile S? In this paper we report the results of a study that serve to clarify this long-standing issue by demonstrating that the nucleophile that promotes migratory insertion to form the acyl intermediate dissociates from the latter prior to its trapping.

This study, which extends our earlier investigations of C–H bond-forming reductive elimination reactions,[4,5] relates to the reaction of p-$CH_3OC_6H_4CH_2Mn(CO)_5$ [abbreviated Bz′Mn(CO)$_5$] with *cis*-$HMn(CO)_4(PMe_2Ph)$ [abbreviated $HMn(CO)_4P$] to form Bz′CHO in accord with eq 4. Previously we have reported

$$Bz'Mn(CO)_5 + cis\text{-}HMn(CO)_4(PMe_2Ph) + CO \rightarrow Bz'CHO + \text{axial-}Mn_2(CO)_9(PMe_2Ph) \quad (4)$$

that the migratory insertion step in this reaction is promoted by donor solvents such as acetone and acetonitrile.[4] Subsequently, we have found that phosphine oxides constitute much more powerful catalysts for this reaction and we now report the results of a kinetic study of reaction 4, catalyzed by triphenylphosphine oxide.[6]

Assuming, in line with earlier interpretations, that the role of $OPPh_3$ is to induce migratory insertion by the associative step (5), two alternative mechanisms may be envisaged for the overall catalytic reaction. These encompass associative and dissociative mechanisms, respectively, for the subsequent trapping of the acyl intermediate by $HMn(CO)_4(PMe_2Ph)$[8] in accord with the following mechanistic schemes and kinetic behavior.

(A) Associative Mechanism

$$Bz'Mn(CO)_5 + OPPh_3 \underset{k_{-5}}{\overset{k_5}{\rightleftharpoons}} \underset{\mathbf{1}}{Bz'C(=O)Mn(CO)_4(OPPh_3)} \quad (5)$$

$$\mathbf{1} + HMn(CO)_4P \xrightarrow{k_6} Bz'CHO + \underset{\mathbf{2}}{Mn_2(CO)_8P} + OPPh_3 \quad (6)$$

$$\mathbf{2} + CO \xrightarrow{\text{fast}} Mn_2(CO)_9P \quad (7)$$

Application of the steady-state approximation to **1** yields the rate law eq 8, which rearranges to eq 9.

$$k_{obsd} = -\mathrm{d}\ln[Bz'Mn(CO)_5]/\mathrm{d}t = \frac{k_5k_6[HMn(CO)_4P][OPPh_3]}{k_{-5} + k_6[HMn(CO)_4P]} \quad (8)$$

$$(k_{obsd})^{-1} = \left(1 + \frac{k_{-5}}{k_6[HMn(CO)_4P]}\right)\frac{1}{k_5[OPPh_3]} \quad (9)$$

(B) Dissociative Mechanism

$$Bz'Mn(CO)_5 + OPPh_3 \underset{k_{-5}}{\overset{k_5}{\rightleftharpoons}} \mathbf{1} \quad (5)$$

$$\mathbf{1} \underset{k_{-10}}{\overset{k_{10}}{\rightleftharpoons}} \underset{\mathbf{3}}{Bz'C(=O)Mn(CO)_4} + OPPh_3 \quad (10)$$

$$\mathbf{3} + HMn(CO)_4P \xrightarrow{k_{11}} Bz'CHO + \mathbf{2} \quad (11)$$

$$\mathbf{2} + CO \xrightarrow{\text{fast}} Mn_2(CO)_9P \quad (7)$$

Application of the steady-state approximation to **1** and **3** yields the rate law eq 12, which rearranges to eq 13.

$$k_{obsd} = \frac{k_5k_{10}k_{11}[HMn(CO)_4P][OPPh_3]}{k_{-5}k_{-10}[OPPh_3] + k_{11}(k_{-5} + k_{10})[HMn(CO)_4P]} \quad (12)$$

$$(k_{obsd})^{-1} = \frac{k_{-5}k_{-10}}{k_5k_{10}k_{11}[HMn(CO)_4P]} + \frac{k_{-5} + k_{10}}{k_5k_{10}[OPPh_3]} \quad (13)$$

According to the *associative* mechanism A linear plots of $(k_{obsd})^{-1}$ vs. $[OPPh_3]^{-1}$ at different $HMn(CO)_4P$ concentrations all should pass through the origin with slopes that depend inversely on $[HMn(CO)_4P]$. In contrast, the *dissociative* mechanism B predicts that the slopes of such plots should be independent of $[HMn(CO)_4P]$ but that they should have nonzero intercepts which are inversely proportional to $[HMn(CO)_4P]$.

Our kinetic measurements on reaction 4 in C_6D_6 at 45 °C, designed to test the validity of the above interpretations, encompassed the initial reactant concentration ranges, 3.8×10^{-3} to 2.4×10^{-2} M Bz′Mn(CO)$_5$, 3.3×10^{-2} to 0.16 M $HMn(CO)_4(PMe_2Ph)$ (typically at least 10-fold excess over Bz′Mn(CO)$_5$), 0.040 to 0.30 M $OPPh_3$, and 1.1 to 2.3 atm (8.1×10^{-3} to 1.7×10^{-2} M) of CO.[9] Under these conditions the reaction exhibited pseudo-first-order kinetics ($-\mathrm{d}\ln[Bz'Mn(CO)_5]/\mathrm{d}t = k_{obsd}$) with

(4) (a) Nappa, M. J.; Santi, R.; Diefenbach, S. P.; Halpern, J. *J. Am. Chem. Soc.* **1982**, *104*, 619. (b) Nappa, M. J.; Santi, R.; Halpern, J. *Organometallics* **1985**, *4*, 34.

(5) Halpern, J. *Acc. Chem. Res.* **1982**, *15*, 332.

(6) The pronounced catalytic influence of phosphine oxides on the migratory insertion of CO was first identified in this laboratory by László Markó and Bernadett Markó-Monostory in a study of the competing reactions Bz′C(=O)Mn(CO)$_5$ → Bz′Mn(CO)$_5$ + CO and Bz′C(=O)Mn(CO)$_5$ + $HMn(CO)_4(PPh_3)$ + CO → Bz′CHO + $Mn_2(CO)_9(PPh_3)$9 The results of this study will be published elsewhere. We also recognize a possible connection between this influence and the substitution labilization of metal carbonyls by phosphine oxides reported by Darensbourg et al.[7]

(7) (a) Darensbourg, D. J.; Walker, N.; Darensbourg, M. Y. *J. Am. Chem. Soc.* **1980**, *102*, 1213. (b) Darensbourg, D. J.; Darensbourg, M. Y.; Walker, N. *Inorg. Chem.* **1981**, *20*, 1918.

(8) $HMn(CO)_4(PMe_2Ph)$ was used to trap the acyl intermediate because its reactivity was sufficiently low to permit observation of the competition between the trapping step (11) and the reverse of reaction (10). For more reactive traps such as HMn(CO)$_5$ or PPh_3 the ratio k_{11}/k_{-10} was too large, and the intercepts of plots such as those in Figure 1 consequently too small, to permit the latter to be identified and the alternative mechanistic schemes A and B to be distinguished.

(9) The reactions were followed by ^1H and ^{31}P NMR and FTIR. This permitted all the reactants and products to be monitored. The formation of $Mn_2(CO)_9P$ was quantitative. The yield of Bz′CHO passed through a maximum (typically ca. 80% of the initial Bz′Mn(CO)$_5$, somewhat higher in the fastest experiments) and then decreased due to side reactions to yield unidentified (probably polymeric) products. Bz′CHO was without effect on the reaction of Bz′Mn(CO)$_5$ with $HMn(CO)_4P$ (confirmed in control experiments). The reactions were conducted under a CO atmosphere (a) to trap $Mn_2(CO)_8(PMe_2Ph)$ and yield a stable identifiable product and (b) to suppress the formation of Bz′H by a side reaction initiated by the reversible loss of CO from Bz′Mn(CO)$_5$.[4]

k_{obsd} independent of the CO concentration. The results, which are reported in Figure 1 in the form of plots of $(k_{obsd})^{-1}$ vs. $[OPPh_3]^{-1}$, clearly conform to eq 13 and provide convincing support for the dissociative trapping mechanism B.[10] The plots in Figure 1 yield the values $(k_{-5}k_{-10})/(k_5k_{10}k_{11}) = (1.36 \pm 0.04) \times 10^2$ M s and $(k_{-5} + k_{10})/(k_5k_{10}) = (2.58 \pm 0.09) \times 10^2$ M s.

According to the mechanistic interpretation of eq 5, 10, 11, and 7, the intercepts of the plots in Figure 1 $(k_{-5}k_{-10}/(k_5k_{10}k_{11})$-$[HMn(CO)_4P])$ correspond to establishment of the equilibrium of eq 14 and trapping of the equilibrium concentration of Bz'C-

$$Bz'Mn(CO)_5 \rightleftarrows Bz'C(=O)Mn(CO)_4 \qquad (14)$$

$(=O)Mn(CO)_4$ (**3**) by $HMn(CO)_4P$. This predicts that the magnitudes of the intercepts of such plots should be independent of the identity of the catalytic nucleophile. Preliminary experiments with other catalysts including $OPBu_3$, CH_3CN, and THF confirm this prediction and support the same mechanistic interpretation of earlier observations of the promotion of CO migratory insertion by other donor solvents and nucleophilic reagents.[2,3] *We conclude that the role of such nucleophiles is not to stabilize the coordinately unsaturated acyl intermediates (e.g., 3) but rather to catalyze their formation.*

Further experiments to determine some of the individual rate constants in eq 12 and to extend these studies to other catalysts and other CO migratory insertion reactions (notably of $CpMo(CO)_3R$ and $CpFe(CO)_2R$) are in progress.

Acknowledgment. We thank the National Science Foundation and the Sun Oil Co. for grants in support of this research. The NMR facilities were supported in part through the University of Chicago Cancer Center Grant NIH-CA-14599.

(10) In the plot of [intercept]$^{-1}$ vs. $[HMn(CO)_4P]^{-1}$ (inset in Figure 1) the point for the lowest $HMn(CO)_4P$ concentration (0.031 M) falls below the line passing through the other points. This is attributable to a contribution from the trapping of **3** by CO which becomes significant under these conditions. In accord with this, up to 10% $Bz'C(=O)Mn(CO)_5$ was observed to form in these experiments; at higher $HMn(CO)_4(PMe_2Ph)$ concentrations the yield of $Bz'C(=O)Mn(CO)_5$ was much lower ($\lesssim$5%). Such additional trapping by CO effectively increases the value of the trapping rate constant k_{11}. In accord with eq 12 and Figure 1, this reduces the intercept of the plot of $(k_{obsd})^{-1}$ vs. $[OPPh_3]^{-1}$ but does not affect the slope. Under the circumstances the point for 0.031 M $HMn(CO)_4P$ was omitted from the calculation of $(k_{-5}k_{-10})/(k_5k_{10}k_{11})$.

Geometrical Characteristics from Experiment and Theory of Isostructural Complexes Involving Palladium– and Platinum–Methyl Bonds

Jean M. Wisner, Tadeusz J. Bartczak, and James A. Ibers*

Department of Chemistry, Northwestern University Evanston, Illinois 60201

John J. Low and William A. Goddard III*

Contribution No. 7169, Division of Chemistry and Chemical Engineering, California Institute of Technology Pasadena, California 91125

Received May 20, 1985

Oxidative addition and reductive elimination reactions play a critical role in some of the most important processes in organometallic chemistry.[1] In such reactions, Pd(II) and Pt(II) systems often show different chemistry. As one example, reductive coupling of C–C bonds from Pd(II)[2]

$$Pd(CH_3)_2(PPh_3)_2 \rightarrow Pd(PPh_3)_2 + C_2H_6$$

(1) Collman, J. P.; Hegedus, L. S. "Principles and Applications of Organotransition Metal Chemistry"; University Science Books: Mill Valley, CA, 1980; Chapter 4.

(2) Gillie, A.; Stille, J. K. *J. Am. Chem. Soc.* **1980**, *102*, 4933–4941. Loar, M. K.; Stille, J. K. *Ibid.* **1981**, *103*, 4174–4181. Moravskiy, A.; Stille, J. K. *Ibid.* **1981**, *103*, 4182–4186. Ozawa, F.; Ito, T.; Nakamura, Y.; Yamamoto, A. *Bull. Chem. Soc. Jpn.* **1981**, *54*, 1868–1880.

Table I. Experimental and Theoretical Bond Distances (Å) in $M(CH_3)_2(PR_3)_2$ Systems

	exptl $M(CH_3)_2[P(C_6H_5)_2CH_3]_2$	theoretical $M(CH_3)_2(PH_3)_2$
⟨Pt–C⟩	2.120 (4)[a]	2.06
⟨Pd–C⟩	2.090 (2)	2.02
Δ_C	0.030 (4)	0.04
⟨Pt–P⟩	2.284 (1)	2.46
⟨Pd–P⟩	2.323 (1)	2.50
Δ_P	−0.039 (1)	−0.04

[a] Estimated standard deviation of the mean.

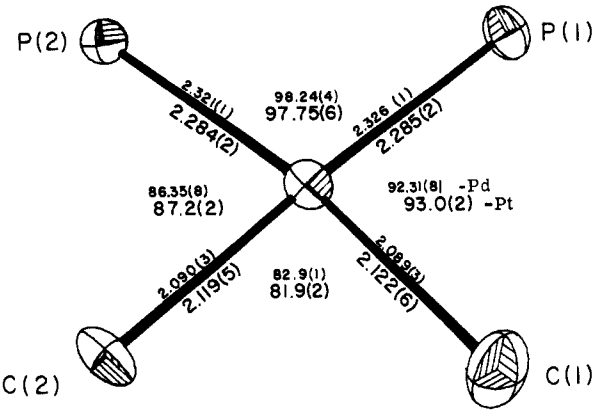

Figure 1. Coordination sphere around the metal in *cis*-$M(CH_3)_2[P(C_6H_5)_2CH_3]_2$, M = Pt, Pd. Bond distances and angles for the Pd complex are in smaller type. Thermal ellipsoids at the 50% probability level are shown.

has been shown to be concerted.[2] However, $Pt(CH_3)_2(PR_3)_2$ complexes are very stable and have never been reported to undergo reductive elimination.[3] Indeed, Pt dialkyls tend to decompose through β-hydride elimination[4] if this pathway is available, even though direct C–C reductive coupling is thermodynamically favored. This dramatically different chemistry for very similar Pd(II) and Pt(II) systems led us to pursue the present experimental and theoretical studies[5] on the geometries and energetics for the species *cis*-$M(CH_3)_2(PR_3)_2$, where M = Pd or Pt.

With an interest in correlating metrical information with reactivity, we undertook an X-ray structural study of the complexes *cis*-$M(CH_3)_2[P(C_6H_5)_2CH_3]_2$, where M = Pd or Pt. Prior to this study, no structural comparisons of Pt and Pd alkyl complexes had been made. In fact, the literature contains only two reports[6] of structures with Pd–Me bonds. The present complexes were chosen because of their relative stability and simplicity. *cis*-$M(CH_3)_2[P(C_6H_5)_2CH_3]_2$, M = Pd or Pt, are strictly isostructural,[7]

(3) Whitesides, G. M.; Gaasch, J. F.; Stedronsky, E. R. *J. Am. Chem. Soc.* **1972**, *94*, 5258–5270. McDermott, J. X.; White, J. F.; Whitesides, G. M. *Ibid.* **1984**, *98*, 6521–6528. Young, G. B.; Whitesides, G. M. *Ibid.* **1978**, *100*, 5808–5815. McCarthy, T. J.; Nuzzo, R. G.; Whitesides, G. M. *Ibid.* **1981**, *103*, 1676–1678; **1981**, *103*, 3396–3403. Nuzzo, R. G.; McCarthy, T. J.; Whitesides, G. M. *Ibid.* **1981**, *103*, 3404–3410. Komiya, S.; Morimoto, Y.; Yamamoto, A.; Yamamoto, T. *Organometallics* **1981**, *1*, 1528–1536.

(4) Chatt, J.; Shaw, B. L. *J. Chem. Soc.* **1959**, 705–716.

(5) Generalized valence bond calculations [involving correlations of all 12 electrons associated with the metal and the bonds to the CH_3 groups] were carried out using relativistic effective core potentials on the Pd and Pt, as described for $Pt(H)_2(PH_3)_2$ in: Low, J. J.; Goddard, W. A., III *J. Am. Chem. Soc.* **1984**, *106*, 6928–6937.

(6) Olmstead, M. M.; Farr, J. P.; Balch, A. L. *Inorg. Chim. Acta* **1981**, *52*, 47–54. Crutchley, R. J.; Powell, J.; Faggiani, R.; Lock, C. J. L. *Inorg. Chim. Acta* **1977**, *24*, L15–L16.

(7) Selected data for the X-ray structure determinations. Pd complex: C_{2h}^5-$P2_1/c$, $Z = 4$, $a = 8.882$ (3) Å, $b = 26.500$ (7) Å, $c = 11.168$ (4) Å, $\beta = 108.27$ (4)°, $V = 2496$ Å^3 at −162 °C. 4799 independent F_o^2 values used to determine 280 variables—all nonhydrogen atoms anisotropic, H atoms, including methyl H atoms located and idealized. $R(F^2) = 0.038$; $R(F)$ for $F_o^2 > 3\sigma(F_o^2) = 0.028$. Pt complex: C_{2h}^5-$P2_1/c$, $Z = 4$, $a = 8.859$ (4) Å, $b = 26.302$ (10) Å, $c = 11.215$ (5) Å, $\beta = 108.60$ (2)°, $V = 2476$ Å^3 at −162 °C. 7678 independent F_o^2, same model as for Pd. $R(F^2) = 0.078$; $R(F) = 0.049$. Details will appear elsewhere: Wisner, J. M.; Bartczak, T. J.; Ibers, J. A., unpublished results.

0002-7863/86/1508-0347$01.50/0